

# Experimental and Theoretical Studies of the Electronic Structure of Poly(*p*-phenylenevinylene) and Some Ring-Substituted Derivatives

M. Fahlman,\* M. Lögdlund, S. Stafström, and W. R. Salaneck

Department of Physics, Linköping University, S-58183 Linköping, Sweden

R. H. Friend

Cavendish Laboratory, University of Cambridge, Cambridge CB3 0HE, United Kingdom

P. L. Burn and A. B. Holmes

University Chemical Laboratory, Lensfield Road, Cambridge CB2 1EW, United Kingdom

K. Kaeriyama and Y. Sonoda

National Institute of Materials and Chemical Research, Tsukuba, Ibaraki 305, Japan

O. Lhost, F. Meyers, and J. L. Brédas

Service de Chimie des Matériaux Nouveaux, Département des Matériaux et Procédés, Université de Mons-Hainaut, B-7000 Mons, Belgium

Received June 24, 1994; Revised Manuscript Received December 12, 1994\*

**ABSTRACT:** The electronic structure of a conjugated polymer of current interest in organic LED's, poly(*p*-phenylenevinylene), or PPV, has been studied by ultraviolet photoelectron spectroscopy and X-ray photoelectron spectroscopy. The focus of this work is on the nature of the  $\pi$ -electronic band structure nearest the Fermi level and the physical influence of finite torsion angles, the geometry of the polymer backbone, on the electronic properties of the system. Details of the  $\pi$ -electronic bands, as reflected in the associated density-of-states, are observed clearly in the spectra, from which some underlying geometrical details of the polymer system can be deduced. The experimental spectra have been analyzed theoretically using band structure calculations based upon the valence effective Hamiltonian (VEH) model. In addition, in order to control the band structure, three ring-substituted derivatives of PPV, each of which induces a different bonding geometry in the backbone, have been studied. The changes in the experimental results can be explained on the basis of both physical and chemical interactions of the substituents with the backbone, which lead to geometrical changes along the backbone, which influence the  $\pi$ -bandwidths and contribute to differences in both the optical absorption threshold and the binding energy of the valence band edge.

## I. Introduction

Since the discovery that polyacetylene can be doped (*i.e.*, chemically oxidized or reduced) to extremely high electrical conductivities,<sup>1</sup> interest in conjugated polymers has continuously increased.<sup>2,3</sup> More recently, much attention has been devoted to the pristine (semi-conducting) state of conjugated polymers, which also exhibit a number of interesting properties. For instance, many conjugated polymers present remarkable third-order nonlinear optical coefficients<sup>4,5</sup> or lend themselves to use as active components in devices such as field-effect transistors<sup>6–8</sup> or light-emitting diodes.<sup>9,10</sup> In this context, poly(*p*-phenylenevinylene) and its alkyl and alkoxy derivatives are the focus of numerous studies. This is because of their good environmental stability and processability, the latter property coming from the availability of soluble-precursor synthetic routes<sup>11,12</sup> or, in the presence of rather long aliphatic tails connected to the phenylene rings, from solubility in common organic solvents.<sup>13,14</sup>

The purpose of this work is to examine in detail, from a joint experimental and theoretical approach, the electronic structure of the poly(*p*-phenylenevinylene)s and, in particular, to understand the influence of alkyl

or alkoxy ring substituents on the top region of the valence band and on the electronic band gap. This is especially important in the context of determining the characteristics of hole injection processes or of light emission in connection with electro- or photoluminescence phenomena. The materials considered here include unsubstituted poly(*p*-phenylenevinylene), or PPV, as well as the following derivatives: (i) poly(2,5-diheptyl-1,4-phenylenevinylene), or DHPPV; (ii) poly(2,5-dimethoxy-1,4-phenylenevinylene), or DMeOPPV; and (iii) poly(2-methoxy-5-(2'-ethylhexoxy)-1,4-phenylenevinylene), or MEHPPV. The molecular structures of these four polymers are illustrated in Figure 1.

A preliminary brief report on some of the experimental spectra appears in the proceedings of ICSM-92.<sup>15</sup> This paper is structured as follows. In section II, the origins of the samples studied experimentally are described and the characteristics of the photoelectron spectrometer are indicated. The theoretical methodology is described in section III. The experimental and theoretical electronic-structure results are presented and discussed in section IV, first in terms of the whole valence band and then in terms of the top two occupied electronic bands. The conclusions are given in section V.

## II. Experimental Details

Films of PPV and DMeOPPV were prepared by spin-coating precursor polymers onto appropriate substrates and converting

\* Abstract published in *Advance ACS Abstracts*, February 1, 1995.

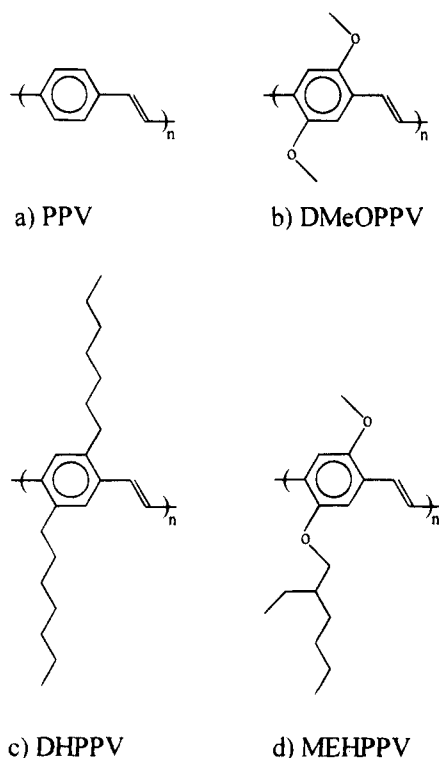


**Figure 1.** Molecular structures of (a) poly(*p*-phenylenevinyl) (PPV), (b) poly(2,5-dimethoxy-1,4-phenylenevinylene) (DMeOPPv), (c) poly(2,5-diheptyl-1,4-phenylenevinylene) (DHPPV), and (d) poly(2-methoxy-5-(2'-ethylhexoxy)-1,4-phenylenevinylene) (MEHPPV).

samples to the conjugated polymers *in situ*, i.e., in the ultrahigh vacuum environment of the photoelectron spectrometer. The PPV used here was prepared from a tetrahydrothiophene "leaving-group precursor polymer", spin-coated from solution in methanol, and converted to PPV at temperatures between 200 and 250 °C *in vacuo*.<sup>16–18</sup> DMeOPPv was prepared by the methanol leaving-group precursor polymer, spin-coated from solution in chloroform, and converted to the conjugated form at temperatures between 200 and 250 °C under flowing argon and HCl.<sup>18–20</sup> MEHPPV was prepared according to literature routes<sup>21</sup> and was spin-coated directly from solution in chloroform. Samples of all three polymers were prepared in Cambridge as thin films (<50 nm) on gold-covered Si substrates and shipped to Linköping sealed in a N<sub>2</sub> atmosphere in glass. Thin films of poly(2,5-diheptyl-1,4-phenylenevinylene) or its precursor, synthesized at the National Institute of Materials and Chemical Research,<sup>14</sup> were prepared in Linköping by spin-coating onto aluminum-covered Si substrates. The precursor samples were thermally converted *in situ* in the ultrahigh vacuum (UHV) chamber of the photoelectron spectrometer.

Both X-ray and ultraviolet photoelectron spectroscopies, XPS and UPS, were carried out in Linköping in an instrument of custom design and construction. The base pressure is about 10<sup>–10</sup> torr. An unmonochromatized Mg Kα<sub>1,2</sub> X-ray source ( $h\nu = 1253.6$  eV) was used for XPS, while UPS was carried out using monochromatized He I ( $h\nu = 21.2$  eV) and He II ( $h\nu = 40.8$  eV) photons. The He II spectra shown have been treated with a three-point smoothing routine.

Examination of the XPS core level spectra shows that the poly(*p*-phenylenevinylene), poly(2,5-dimethoxy-1,4-phenylenevinylene), and poly(2-methoxy-5-(2'-ethylhexoxy)-1,4-phenylenevinylene) samples are all free from significant oxygen contamination. On the contrary, the samples of poly(2,5-diheptyl-1,4-phenylenevinylene) do contain some oxygen contamination, about one oxygen atom per two monomer units. From both the XPS and UPS spectra, it seems that the oxygen is not directly associated with the PPV polymer chains and may thus occur in the form of a molecular impurity, for example, as encapsulated water molecules.

### III. Theoretical Methodology

The electronic band structure calculations were carried out on isolated polymer chains using the valence effective Hamiltonian model.<sup>22,23</sup> The VEH method is a nonempirical pseudopotential method based on the use of an effective Fock Hamiltonian. The parameters of the atomic potentials are determined by comparison with Hartree–Fock *ab initio* double- $\zeta$  calculations of the electronic structure of model molecules.<sup>22</sup> The merits of the VEH technique and, in particular, its successful application to simulate the XPS or UPS valence band spectra of a wide range of conjugated materials have been well described in the literature.<sup>24–27</sup>

The bare density-of-valence-electronic-states (DOVS) curves are directly computed in the conventional way by taking the inverse of the derivative of the electronic band structure with respect to momentum. In order to make the comparison with the solid-state UPS data, the bare DOVS curves are then submitted to a standard threefold procedure: (i) a *contraction* on the energy scale by a factor of 1/1.3; (ii) a *shift* to lower binding energies; and (iii) a *convolution* by a Gaussian, the full width at half-maximum of which is taken to be 0.7 eV. The contraction is required because the parameters used in VEH are based on Hartree–Fock calculations, which are known to produce full valence bandwidths that are too wide (note that the 1/1.3 factor has been used systematically in VEH calculations and is not adjusted). The energy shift is necessary because the calculations are performed on a single isolated polymer chain and, therefore, do not take into account uniform intermolecular relaxation (polarization) energy effects which occur in the solid state.<sup>24,28</sup> The numerical value of the energy shift, 3.3 eV, has been set in order to match the calculated DOVS curves to the UPS experimental at the lowest binding energy peak position for unsubstituted PPV and then has been taken to be the same (not adjusted) for all of the other polymers. This approximation, which is equivalent to assuming that the electronic screening in the UPS spectra is constant among the materials studied here, is rational, given the chemical similarities of the samples studied. The convolution allows one to simulate the experimental resolution as well as the peak broadening that is often present in the solid state, namely, interchain interactions and disorder effects.

The molecular geometries used as input for the electronic bandstructure calculations were obtained via Hartree–Fock semiempirical Austin Model 1 (AM1)<sup>29</sup> geometry optimization calculations. The AM1 method is known to yield good estimates of the geometry for organic molecules; in terms of conformational analysis, it is much superior to its predecessor, MNDO (modified neglect of diatomic overlap<sup>30</sup>) and gives very good agreement with respect to *ab initio* results (see, for example, refs 31 and 32). The geometry optimization was carried out on oligomers, the central parts of which were used as unit cells for the polymers.

### IV. Results and Discussion

**(a) Full Valence Band Spectra.** The valence XPS and UPS spectra of poly(*p*-phenylenevinylene) have been reported previously in the literature (see, for example, refs 15 and 33–37). However, in order to better appreciate the influence of substituents, it is judged to be useful to repeat the UPS theoretical and experimental spectra for PPV here, for comparison with the spectra for the substituted PPV's.

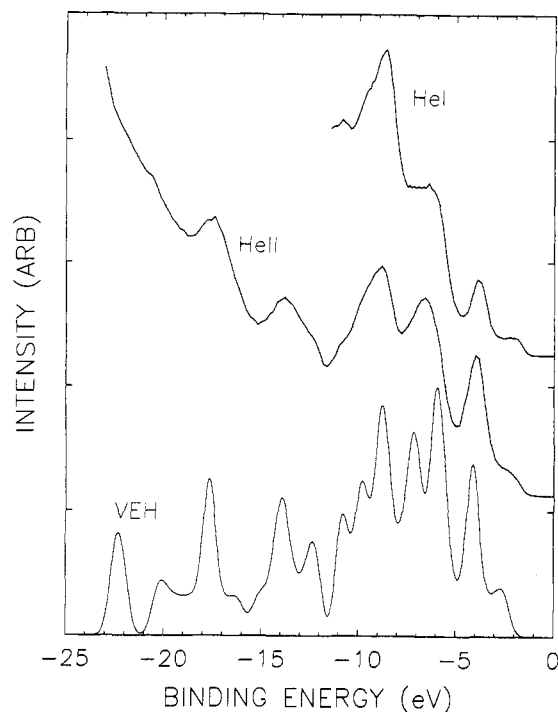


**Figure 2.** He I and He II UPS spectra of PPV and the corresponding VEH DOVS curve.

Recent Hartree-Fock *ab initio* and AM1 calculations performed on the isolated stilbene molecule (which corresponds to the phenyl-capped monomer unit of PPV) have indicated<sup>31</sup> that, in the gas phase, there is a very flat potential, for the torsion angle of the phenyl rings out of the plane of the vinylene linkage, extending between about  $+30^\circ$  and  $30^\circ$ . Neutron-diffraction data on oriented PPV samples show that, at room temperature in the solid state, the ring torsion angles are  $7 \pm 6^\circ$ .<sup>38</sup> Such a small value of the torsion angle results in negligible effects on the electronic band structure, with respect to a fully coplanar conformation, in the VEH results. Therefore, the results of the VEH calculations presented here are for planar PPV.

The VEH-calculated DOVS spectrum of unsubstituted PPV is compared with the experimental He I and He II spectra in Figure 2.<sup>37</sup> Excellent agreement is found between theory and experiment, both for spectral peak positions and intensities. The VEH band gap,  $E_g$ , is calculated to be 2.3 eV. From optical absorption spectra, the maximum of the first absorption peak in well-oriented PPV samples is 2.5 eV.<sup>39</sup> In the UPS spectra, the energy difference between the observed  $\pi$ -band edge and the Fermi energy (which is the reference level in the presentation of the spectra) should be equal to half the optical band gap, when the Fermi level falls exactly at the center of the band gap, as in an intrinsic undoped semiconductor. The experimental UPS spectra indicate  $E_g$  to be slightly less than 3.0 eV, in reasonably good agreement with the value obtained directly from optical measurements. The slight difference between the expected and measured values is partially due to the difficulty in evaluating accurately the location of the edge of the lowest binding energy feature which has low intensity and partially due to the fact that the presence of even a very slight number of defects could influence the position of the Fermi level by a few tenths of an electronvolt in the undoped samples. A detailed analysis of the relation between the band structure and the valence density of states has been provided in ref 37.

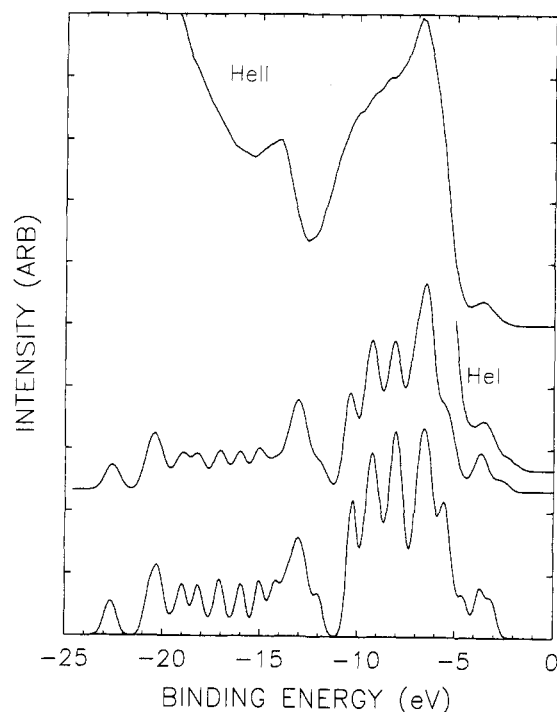


**Figure 3.** He I and He II UPS spectra of DHPPV and corresponding VEH DOVS curves calculated for a coplanar conformation ( $\theta = 0^\circ$ ) and a twisted conformation (ring torsion angles  $\theta = 34^\circ$ ).

In ref 36, a UPS valence band of PPV was presented and analyzed with the help of the results of local density approximation (LDA) calculations. In the experimental spectrum, the  $\pi$ -band edge at about 2 eV in Figure 2, which is the main topic of discussion in this paper, is not resolved. The LDA results fit to the remainder of the UPS spectrum shown. The lowest binding energy feature in the LDA results, corresponding to the  $\pi$ -band edge, were associated with the 4 eV peak instead of the 2 eV peak. Since the focus of the present work is on the valence band edge at 2 eV, the LDA results will not be compared in detail.

Turning to poly(2,5-diheptyl-1,4-phenylenevinylene), the results of AM1 geometry optimization indicate a torsion angle  $\theta$  of  $34^\circ$ , between the plane of the phenyl ring and that of the vinyl bridge. In addition, the geometry of the DHPPV oligomers was optimized under the constraint that the torsion angle  $\theta$  was equal to zero, that is, in a forced planar geometry. Using these AM1 geometry results as input into VEH band structure calculations yields estimates of the optical band gap of  $E_g = 3.2$  eV (for  $\theta = 0^\circ$ ) and  $E_g = 4.3$  eV (for  $\theta = 34^\circ$ ). These values of the band gap are about 1–2 eV larger than what is found experimentally in unsubstituted PPV. In Figure 3, the theoretical DOVS curves of DHPPV, calculated on the basis of both types of geometry ( $\theta = 0^\circ$  and  $34^\circ$ ), are compared with the experimental He I and He II UPS spectra. The band gap inferred from the UPS spectra is found to vary slightly among the samples studied, ranging between about 3.0 and 4.0 eV. This variation in band gap is attributed to changes in the effective  $\pi$ -conjugation length associated with sample-dependent torsion angle variations. The experimental spectra shown in Figure 3 are typical of those samples presenting the lowest average torsion angles; *vide infra*.

By comparing the theoretical DOVS of DHPPV with that of unsubstituted PPV, the effects caused by the ring

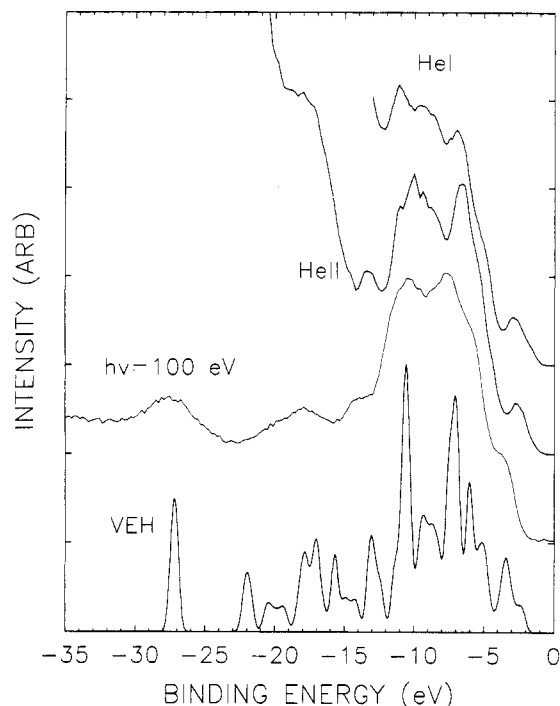


**Figure 4.** He I, He II, and  $h\nu = 100$  eV UPS spectra of DMeOPPV and the corresponding VEH DOVS curve.

addition of the heptyl groups can be studied in more detail. The intensities of the two peaks in the DOVS closest to the band gap (at lowest binding energy), relative to the intensities of the remainder of the DOVS curves, are much lower for DHPPV than for PPV. The heptyl groups contribute only  $\sigma$ -bands, many of which appear in the region between  $-6$  and  $-11$  eV in binding energy, a feature similar to what is found in the poly(alkylthiophene)s.<sup>40</sup> This strongly increases the intensities of the peaks in that energy range, especially the peak at  $-7$  eV. The two lowest binding energy peaks, however, still consist of  $\pi$ -bands related to the backbone. In addition, a number of new features associated with the  $\sigma$ -bands of the heptyl groups appear between  $-12$  and  $-20$  eV, as can be seen by comparison to the spectrum of unsubstituted PPV.

In Figure 4, the calculated DOVS curves of poly(2,5-dimethoxy-1,4-phenylenevinylene) (DMeOPPV) are compared to the He I and He II UPS spectra. The band gap estimated from the UPS data is about 2.5 eV, to be compared to a VEH value of 2.0 eV. The value obtained by optical absorption is  $E_g = 2.15$  eV.<sup>41</sup> AM1 geometry optimization indicates that the isolated polymer chain is in a planar conformation; the planarity is due to the formation hydrogen-type bonding between the oxygen atoms of the methoxy groups and the nearest hydrogens of the adjacent vinylene moieties.<sup>31</sup>

Compared with that of PPV, the theoretical spectrum of DMeOPPV contains a new feature between  $-27$  and  $-28$  eV, which corresponds to the presence of two flat oxygen-2s-derived  $\sigma$ -bands. The oxygen atoms in the methoxy groups also contribute to the intense peaks around  $-11$  eV (oxygen lone pair electrons) and  $-7$  eV (upper energy levels of the methyl groups), which again results in a decrease in the relative intensities of the two  $\pi$ -band peaks closest to the Fermi energy.

The electronic structure of poly(2-methoxy-5-(2'-ethylhexoxy)-1,4-phenylenevinylene) is comparable to that in DMeOPPV. The backbone of the isolated polymer chain is calculated to be in a planar conformation. In

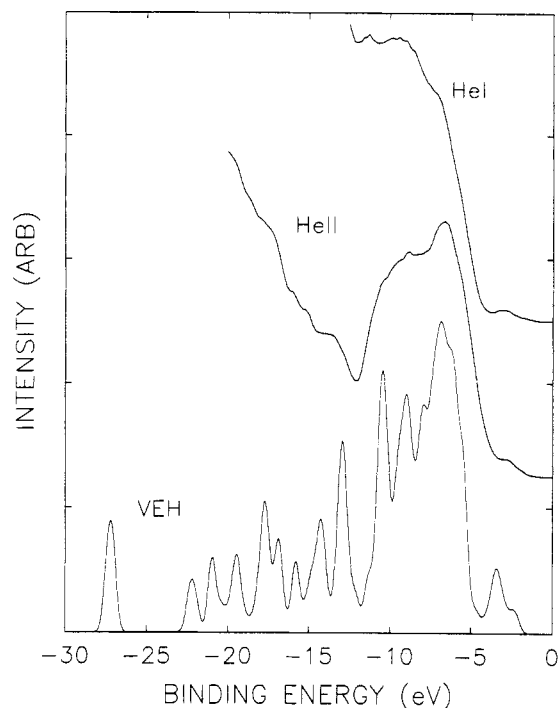


**Figure 5.** He I and He II UPS spectra of MEHPPV and the corresponding VEH DOVS curve.

Figure 5 are displayed the calculated DOVS curves for MEHPPV together with the experimental He I and He II UPS spectra. The band gap estimated from the UPS data and the calculated VEH band gap are the same as for DMeOPPV, *i.e.*, 2.5 and 2.0 eV, respectively. The major difference in the DOVS curves between MEHPPV and DMeOPPV derives from the larger size of the alkyl groups in the former case, which leads to a very intense peak at about  $-7$  eV, as in the case of DHPPV. This feature is clearly observed in the experimental data.

As can be observed from Figures 2–5, the calculated DOVS spectra are in excellent agreement with the experimental UPS spectra with regard to both peak locations and intensities. Therefore, the calculations are able to provide a consistent interpretation of the major differences appearing in the UPS spectra as a function of substitution. Note, however, that the agreement is generally somewhat slightly less good at higher binding energies, where relative photoionization cross-section effects, which are not included in the VEH DOVS curves, affect the UPS spectra. It also is clear that the VEH calculations also provide good estimates of the band gaps when compared to the optical absorption data. In the UPS spectra, the energy difference between the observed  $\pi$ -band edge and the Fermi energy should provide a rough estimate of half the band gap, which also is in very good agreement with the results of optical studies. With substituents at the 2 and 5 positions of the PPV phenylene rings, the most interesting changes in the electronic structure of PPV are those which occur close to the valence band edge, which will be discussed in detail in the following section.

**(b) Upper Valence Band Spectra.** To illustrate more directly the origins of the effects to be discussed, the structure in the UPS He I spectra closest to the valence band edge is compared directly with the two highest occupied  $\pi$ -bands obtained from the VEH band structure calculations in Figures 6–8. In all cases, the highest occupied band is the fourth  $\pi$ -band, denoted  $4\pi$ , which is derived from electronic states delocalized along

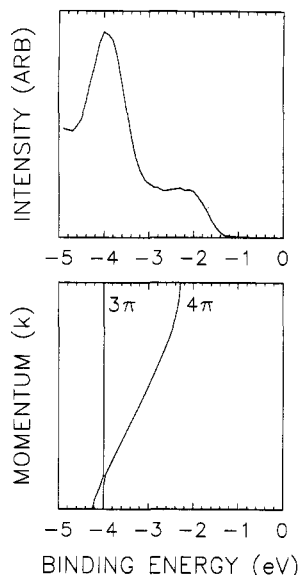


**Figure 6.** Top part of the He I UPS spectrum and VEH upper two occupied  $\pi$ -bands for PPV.

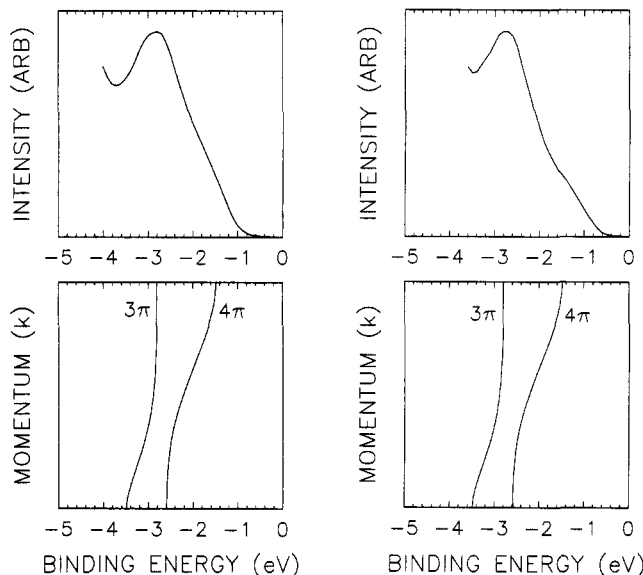


**Figure 8.** Top part of the He I UPS spectrum and VEH upper two occupied bands for (a, left) DMeOPPV and (b, right) MEHPPV.

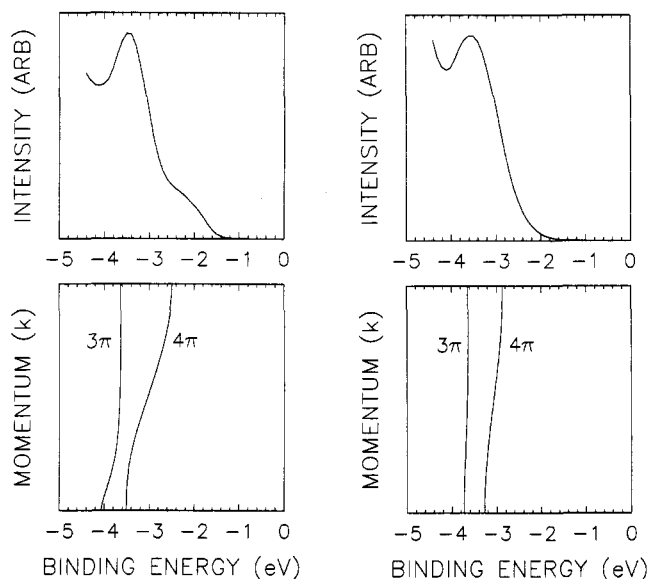


**Figure 7.** Top part of the He I UPS spectrum and VEH upper two occupied  $\pi$ -bands for DHPPV: (a, left) coplanar conformation; (b, right) twisted ( $\theta = 34^\circ$ ) conformation.

the polymer backbone. The top of this band has almost equal contributions from the electronic wave functions of the phenylene rings and the vinylene linkages. The second highest occupied band is the flat  $3\pi$  band, derived from electronic states that are localized on the phenylene rings. The origin of these two  $\pi$ -bands in terms of LCAO coefficients has been discussed *e.g.* in ref 37.

In the case of unsubstituted PPV, illustrated in Figure 6, an avoided crossing between the two bands occurs because of the symmetry within the unit cell. In the experimental spectrum, the difference between the locations of the two peaks with lowest binding energies reflects the difference between the top part of band  $4\pi$  and the flat  $3\pi$  band, *i.e.*, about 1.8 eV. It should be noted that the flat band appears only 0.2 eV above what would constitute the bottom part of the wide band in the absence of an avoided crossing.

As mentioned previously, steric hindrance occurs between the hydrogen atoms on the vinyl bridges and the heptyl groups on the phenylene rings along the

chain axis of DHPPV. These interactions force the rings to twist out of the plane of the backbone, with the optimal torsion angle being  $34^\circ$  at the AM1 level. From the AM1 results, the potential barrier toward a coplanar conformation is about 2.3 kcal/mol per ring and is relatively flat around the minimum. Thus solid-state packing effects can be expected to drive the conformation toward a more coplanar configuration, at least in the better ordered samples. In such a case,  $\pi$ -electron delocalization along the backbone will be at its maximum and lead to a dispersed  $4\pi$  band. Large ring torsions would, on the contrary, decrease the overlap and, as a consequence, diminish the  $4\pi$  bandwidth and increase both the ionization potential and the band gap.

There were significant apparent variations in the position of the  $\pi$ -band edge (and the optical absorption edge) among the DHPPV samples examined. These variations are ascribed to variations in the average ring torsion angle. In general, the DHPPV samples made by converting the precursor polymer in Linköping had a larger optical band gap (larger average torsion angle) than the DHPPV samples converted in Tsukuba. Smaller variations occurred within each of the two sample groups. This sensitivity to sample preparation is an indication that the degree of order, and thus the influence of solid-state packing, is different in different samples.

In Figure 7, the calculated  $3\pi$  and  $4\pi$  bands are shown for DHPPV, both in a coplanar conformation and in a conformation with ring torsion angles of  $34^\circ$ . In the former case Figure 7a, there is very good agreement with one of the UPS spectra taken on a DHPPV sample converted in Tsukuba, indicating that in this particular film the polymer backbones appear to be approximately coplanar. As is evident from the figure, there are effects of the heptyl groups on the electronic structure of the upper part of the valence band, mainly the position of the flat  $3\pi$  band. The flat band is shifted upward by about 0.4 eV in comparison with that of PPV. According to the VEH wave functions, this shift corresponds to antibonding interactions between the first carbon of the aliphatic chain and the ring ortho carbon to which it is attached. The total width of the two bands (2.0 eV) and

the ionization potential are the same as for unsubstituted PPV. The shift of the flat band is in good agreement with the shift of the main peak in the UPS spectrum, to  $-3.5$  eV up from  $-4.0$  eV in PPV. In Figure 7b, the UPS spectrum of another DHPPV sample, converted from the precursor in Linköping, is shown and compared to the calculated energy bands of twisted DHPPV ( $34^\circ$  torsion angle). The total dispersion of the two bands is reduced to  $0.8$  eV. The ionization potential increases by  $0.8$  eV relative to unsubstituted PPV, and to coplanar DHPPV as well. This explains the observation of only one, but clearly broadened, UPS peak nearest the Fermi energy. The other samples of DHPPV studied were found to vary between these two extremes. As yet, no systematic study has been done to optimize the sample preparation process in order to control the average effective torsion angle in a given sample. However, improvements in the sample preparation process have been made to the point where the vast majority of the samples prepared are now in a roughly coplanar configuration.

The upper two calculated energy bands of DMeOPPV and MEHPPV are compared with the corresponding UPS spectra in Figure 8. Here we observe that the oxygen atoms strongly destabilize the highest two occupied bands (which are identical in the two compounds), the flat parts of the two bands being pushed up approximately  $1.2$ – $1.4$  eV compared with the results for unsubstituted PPV. This destabilization is explained by the antibonding character of the interaction between the phenyl ring and methoxy wave functions for the two bands.<sup>41</sup> However, the effect is more pronounced for the  $3\pi$  band, especially for the case of coplanar DHPPV.

The avoided crossing between the two bands increases due to the presence of the alkoxy groups, causing an even larger separation of the two bands.<sup>41</sup> The flat parts of the  $4\pi$  and  $3\pi$  bands lead to a broader peak in the calculated DOVS compared to that for DHPPV and PPV, which is in excellent agreement with the experimental spectra. Because of this broadening, the peak closest to the Fermi energy (that was observed in PPV and DHPPV) is unresolved in the experimental spectrum of DMeOPPV and only slightly perceptible in MEHPPV. However, the total width of the two bands remains  $2$  eV, which suggests the existence of coplanar conformations. This is expected, since for DMeOPPV and MEHPPV, the hydrogen bond type interactions between the oxygen atoms in the alkoxy groups and the hydrogen atoms in the vinyl groups tend to lock the polymer backbone into a coplanar conformation.<sup>31</sup>

The calculated  $\pi$ -bands of DMeOPPV and MEHPPV are found to be essentially identical. This is expected, since the difference in lengths of the alkyl groups between these two compounds affects the  $\sigma$ -bands at higher binding energies and can only affect the characteristics of the upper  $\pi$ -bands if they induce different ring torsion angles along the backbone. This is not the case for DMeOPPV and MEHPPV, however, since the oxygen atoms form hydrogen-type bonds with the vinyl hydrogens, locking these polymers into planar geometries as mentioned previously. Based on these results, the length of the alkyl chains in the alkoxy groups is seen to have little effect on the electronic structure near the Fermi energy, although it can influence the solubility and thermal stability properties of the polymers. The overall agreement with the calculated DOVS with the UPS spectra indicates that there are no major solid-

state effects which negate the results of the calculations carried out on isolated chains.

## V. Synopsis

The electronic structures of PPV, DHPPV, DMeOPPV, and MEHPPV have been studied experimentally by means of ultraviolet and X-ray photoelectron spectroscopies and theoretically using AM1 and VEH quantum-chemical calculations. The densities-of-states obtained from the calculations are in excellent agreement with the UPS spectra. In particular, the agreement in the evolution in energy shifts, bandwidths, and band separation calculated for the different substituents allows the detailed interpretation of the experimental data, as follows:

In the case of PPV, DMeOPPV, and MEHPPV, the theoretical DOVS curves obtained from calculations on isolated chains in coplanar conformations match essentially exactly the experimental UPS data. This fact indicates that solid-state effects do not have a large influence on the electronic structure of the materials, the polymer backbones remaining essentially coplanar at room temperature. On the other hand, for DHPPV, solid-state effects do have a marked impact on the electronic structure near the Fermi energy. Our analysis leads to the conclusion that the variations observed in different samples are caused by solid-state-packing-induced variations in the ring torsion angles.

The ring substituents can affect the characteristics of the upper two  $\pi$  valence bands in two basic ways. The substituents can directly affect the two  $\pi$ -bands by antibonding (bonding) type interactions between the side groups and the phenyl ring, leading to shifts up (down) in energy of the bands. The energy positions of one of the  $\pi$ -bands (the flat  $3\pi$  band) in DHPPV and of the two  $\pi$ -bands in the alkoxy derivatives are affected in this manner. However, the total width of the two bands remains the same as in PPV due to the existence of coplanar conformations.

The substituents also can indirectly affect the highest lying  $\pi$ -bands. The presence of the substituents can lead to modifications of the ring torsion angles along the backbone, either by inducing increased torsion due to steric hindrance between the side groups and the vinyl hydrogens, as is the case in some of the DHPPV, or by locking the geometry into a coplanar configuration due to hydrogen-type bonds between the side groups and vinyl hydrogens, as is the case for DMeOPPV and MEHPPV. The dispersion of the highest occupied band ( $4\pi$ ) is at its maximum for a coplanar configuration and is reduced with increasing torsion angle. Therefore, the addition of substituents to the polymer can be used to tune the highest lying bands in order to optimize the charge injection process in LED's as well as improve the environmental stability and processability of the polymer.

**Acknowledgment.** S. C. Graham, D. A. Halliday, and A. R. Brown in the Cavendish Laboratory are acknowledged for their assistance, and D. D. C. Bradley is acknowledged for many useful discussions. The Linköping–Mons and Mons–Cambridge collaborations are supported by the Commission of the European Community, within the SCIENCE program (Project 0661 POLYSURF) and the BRITE/EURAM program (Project 0148 NAPOLEO), the ESPRIT program (Project 8013 LEDFOS), and the ESPRIT network of excellence NEOME, respectively. The Linköping–RIPT collabora-

tion is supported by the Swedish Board for Technical Development (NuTek). In addition, research on conjugated polymers in Linköping is supported in general by grants from the Swedish Natural Sciences Research Council (NFR), the Swedish National Technical Research Board (TFR), the Neste Corp., Finland, and Philips, NL. The work in Mons is supported by the Prime Minister Office of Science Policy (SPPS) "Pôle d'Attraction Interuniversitaire en Chimie Supramoléculaire et Catalyse" and "Programme d'Impulsion en Technologie de l'Information" (Contract SC/IT/22), by the Belgian National Fund for Scientific Research (FNRS/FRFC), and by an IBM Academic Joint Study.

## References and Notes

- Chiang, C. K.; Fincher, C. R.; Park, Y. W.; Heeger, A. J.; Shirakawa, H.; Louis, E. J.; Gau, S. C.; MacDiarmid, A. G. *Phys. Rev. Lett.* **1977**, *39*, 1098.
- Salaneck, W. R.; Lundström, I.; Rånby, B. *Conjugated Polymers and Related Materials*; Oxford University Press: New York, 1993.
- Brédas, J. L.; Silbey, R., Eds. *Conjugated Polymers: The Novel Science and Technology of Highly Conducting and Nonlinear Optically Active Materials*; Kluwer: Dordrecht, 1991.
- Heeger, A. J.; Orenstein, J.; Ulrich, D. R., Eds. *Nonlinear Optical Properties of Polymers*; Materials Research Society: Pittsburgh, 1988.
- Brédas, J. L.; Chance, R. R., Eds. *Conjugated Polymeric Materials: Opportunities in Electronics, Optoelectronics, and Molecular Electronics*; Kluwer: Dordrecht, 1990.
- Burroughes, J. H.; Friend, R. H. In ref 3, p 555. Burroughes, J. H.; Jones, C. A.; Friend, R. H. *Nature* **1988**, *335*, 137.
- Assadi, A.; Svensson, C.; Willander, M.; Inganäs, O. *Appl. Phys. Lett.* **1988**, *53*, 195.
- Garnier, F.; Horowitz, G.; Peng, X.; Fichou, D. *Adv. Mater.* **1990**, *2*, 592.
- Burroughes, J. H.; Bradley, D. D. C.; Brown, A. R.; Marks, R. N.; Mackay, K.; Friend, R. H.; Burns, P. L.; Holmes, A. B. *Nature* **1990**, *347*, 539. Burn, P. L.; Holmes, A. B.; Kraft, A.; Bradley, D. D. C.; Brown, A. R.; Friend, R. H.; *Nature* **1992**, *356*, 47.
- Braun, D.; Heeger, A. J. *Appl. Phys. Lett.* **1991**, *58*, 1982. Gustafsson, G.; Cao, Y.; Treacy, G. M.; Klavetter, F.; Colaneri, N.; Heeger, A. J. *Nature* **1992**, *357*, 477.
- Gagnon, D. R.; Capistran, J. D.; Karasz, F. E.; Lenz, R. W. *Polym. Bull.* **1984**, *12*, 293.
- Bradley, D. D. C. *J. Phys.* **1987**, *D20*, 1389 and references therein.
- Shi, S.; Wudl, F. *Macromolecules* **1990**, *23*, 2119; *idem*, in ref 5, p 83.
- Sonoda, Y.; Kaeriyama, K. *Bull. Chem. Soc. Jpn.* **1992**, *65*, 853.
- Fahlman, M.; Lhost, O.; Meyers, F.; Brédas, J. L.; Graham, S. C.; Friend, R. H.; Burn, P. L.; Holmes, A. B.; Kaeriyama, K.; Sonoda, Y.; Lögdlund, M.; Stafström, S.; Salaneck, W. R. *Synth. Met.* **1993**, *55–57*, 263.
- Colaneri, N. F.; Bradley, D. D. C.; Friend, R. H.; Burn, P. L.; Holmes, A. B.; Spangler, C. W. *Phys. Rev. B* **1990**, *42*, 11671.
- Burn, P. L.; Bradley, D. D. C.; Brown, A. R.; Friend, R. H.; Holmes, A. B.; Kraft, A.; Martens, J. H. F. *Springer Series in Solid-State Sciences* **1992**, *107*, 293.
- Burn, P. L.; Bradley, D. D. C.; Friend, R. H.; Halliday, D. A.; Holmes, A. B.; Jackson, R. W.; Kraft, A. M. *J. Chem. Soc., Perkin Trans. 1* **1992**, 3225.
- Halliday, D. A.; Bradley, D. D. C.; Burn, P. L.; Friend, R. H.; Holmes, A. B. *Synth. Met.* **1991**, *41–43*, 931.
- Woo, H. S.; Graham, S. C.; Bradley, D. D. C.; Friend, R. H.; Burn, P. L.; Holmes, A. B. *Phys. Rev. B* **1992**, *46*, 7379.
- Wudl, F.; Allemand, P. M.; Srdanov, G.; Ni, Z.; McBranch, D. *ACS Symp. Ser. (Material for Nonlinear Optics)* **1991**, *455*, 683.
- Brédas, J. L.; Chance, R. R.; Silbey, R.; Nicolas, G.; Durand, Ph. *J. Chem. Phys.* **1981**, *75*, 255.
- André, J. M.; Delhalle, J.; Brédas, J. L. *Quantum Chemistry Aided Design of Organic Polymers*; World Scientific: Singapore, 1991.
- Salaneck, W. R. *CRC Crit. Rev. Solid State Mater. Sci.* **1985**, *12*, 267.
- Brédas, J. L.; Chance, R. R.; Silbey, R.; Nicolas, G.; Durand, Ph. *J. Chem. Phys.* **1981**, *77*, 371.
- Brédas, J. L.; Salaneck, W. R. *J. Chem. Phys.* **1986**, *85*, 2219. Kowalczyk, S. P.; Stafström, S.; Brédas, J. L.; Salaneck, W. R.; Jordan-Sweet, J. L. *Phys. Rev. B* **1990**, *41*, 1645.
- Orti, E.; Brédas, J. L. *J. Chem. Phys.* **1988**, *89*, 1009; *J. Am. Chem. Soc.* **1992**, *114*, 8669.
- Sato, N.; Seki, K.; Inokuchi, H. *J. Chem. Soc., Faraday Trans. 2* **1981**, *77*, 1621.
- Dewar, M. J. S.; Zoebish, E. G.; Healy, R. F.; Stewart, J. J. P. *J. Am. Chem. Soc.* **1985**, *107*, 3902.
- Dewar, M. J. S.; Thiel, W. *J. Am. Chem. Soc.* **1977**, *99*, 4899.
- Lhost, O.; Brédas, J. L. *J. Chem. Phys.* **1992**, *96*, 5279.
- Fredriksson, C.; Brédas, J. L. *J. Chem. Phys.* **1993**, *98*, 4253.
- Obrzut, J.; Obrzut, M. J.; Karasz, F. E. *Synth. Met.* **1989**, *29*, E109.
- Seki, K.; Asada, S.; Mori, T.; Inokuchi, H.; Murase, I.; Ohnishi, T.; Noguchi, T. *Solid State Commun.* **1990**, *74*, 677.
- Sato, N.; Lögdlund, M.; Lazzaroni, R.; Salaneck, W. R.; Brédas, J. L.; Bradley, D. D. C.; Friend, R. H.; Ziemelis, K. E. *Chem. Phys.* **1992**, *160*, 299.
- Gomes Da Costa, P.; Dandrea, R. G.; Conwell, E. M.; Fahlman, M.; Lögdlund, M.; Stafström, S.; Salaneck, W. R.; Graham, S. C.; Friend, R. H.; Burn, P. L.; Holmes, A. B. *Synth. Met.* **1993**, *55–57*, 4320.
- Lögdlund, M.; Salaneck, W. R.; Meyers, F.; Brédas, J. L.; Arbuckle, G. A.; Friend, R. H.; Holmes, A. B.; Froyer, G. *Macromolecules* **1993**, *26*, 3815.
- Mao, G.; Fischer, J. E.; Karasz, F. E.; Winokur, M. J. *J. Chem. Phys.* **1993**, *98*, 712.
- Woo, H. S.; Lhost, O.; Graham, S. C.; Bradley, D. D. C.; Friend, R. H.; Quattrocchi, C.; Brédas, J. L.; Schenk, R.; Müllen, K. *Synth. Met.* **1993**, *59*, 13.
- Salaneck, W. R.; Inganäs, O.; Thémans, B.; Nilsson, J. O.; Sjögren, B.; Österholm, J. E.; Brédas, J. L.; Svensson, S. *J. Chem. Phys.* **1988**, *89*, 4613.
- Meyers, F.; Heeger, A. J.; Brédas, J. L. *J. Chem. Phys.* **1992**, *97*, 2750.

MA9412896